

# Quantifying the formation of chiral luminescent lanthanide assemblies in aqueous medium through chiroptical spectroscopy and generation of luminescent hydrogels

Samuel J. Bradberry,<sup>a</sup> Aramballi Jayant Savyasachi,<sup>a</sup> Robert D. Peacock<sup>b</sup> and Thorfinnur Gunnlaugsson<sup>a\*</sup>

<sup>a</sup> *School of Chemistry and Trinity Biomedical Sciences Institute, Trinity College Dublin, University of Dublin, Dublin 2, Ireland*

Fax: + 353 1 671 2826; Tel: + 3531 896 3459; [gunnlaut@tcd.ie](mailto:gunnlaut@tcd.ie)

<sup>b</sup> *School of Chemistry, University of Glasgow, Glasgow, G12 8QQ, Scotland, UK*

**Supporting Information**

## General Experimental Details

Chemicals were purchased from commercial suppliers: Sigma-Aldrich Ireland Ltd., TCI Europe Ltd and Acros Organics and were used, unless stated, used without further purification. Synthesis was completed, unless stated, under inert atmospheres of N<sub>2</sub> or Ar. All microwave reactions were carried out in 2–5 mL or 10–20 mL Biotage Microwave Vials in a Biotage Initiator Eight EXP microwave reactor.

NMR solvents were purchased per-deuterated from Apollo Scientific. Silica chromatography was carried out on a Teledyne Isco CombiFlash automated machine using pre-packed RediSep® cartridges. Thin Layer Chromatography (TLC) was run using Merck Kiesegel 60 F<sub>254</sub> silica plates and visualised under UV irradiation ( $\lambda = 254$  nm) and ethanolic ninhydrin staining. Melting points were determined using an Electrothermal IA900 digital apparatus. NMR was recorded using either an Agilent DD2/LH spectrometer, at 400.1 MHz and 100.6 MHz for <sup>1</sup>H and <sup>13</sup>C experiments, respectively; or a Bruker AV-600 spectrometer at 600.1 MHz and 150.2 MHz for <sup>1</sup>H and <sup>13</sup>C experiments, respectively.

Electrospray mass spectrometry was completed using a Mass Lynz NT V 3.4 on a Waters 600 controller with 996 photodiode array detector. HPLC grade solvents were used throughout and accurate molecular weights determined *via* a peak-matching method against enkephaline standard reference ( $m/z = 556.2771$ ); all accurate masses were reported within  $\pm 5$  ppm of the calculated mass. Infrared spectra were recorded on a Perkin Elmer Spectrum One FT-IR spectrometer fitted with a universal ATR sampling accessory. Circular dichroism absorbance spectroscopy was recorded on a Jasco J-810-150S spectropolarimeter under N<sub>2</sub> flow.

UV-visible absorption spectra were recorded using a Varian Cary 50 spectrophotometer, with applied baseline correction, and luminescence spectra were recorded using a Varian Cary Eclipse spectrophotometer. Spectroscopic grade solvents (Sigma-Aldrich®) were used in quartz cells provided by HellmaAnalytics with path length 10mm.

## Synthetic Experimental

### 4-Hydroxy-*N,N'*-bis(1-(naphthalen-1-yl)ethyl)pyridine-2,6-dicarboxamide (3)

A solution of chelidamic acid monohydrate (0.50 g, 2.49 mmol), HOBt hydrate (0.98 g, 7.25 mmol), EDCI (0.9 mL, 5.10 mmol) and TEA (0.7 mL, 5.02 mmol) in anhydrous THF (50 mL) was stirred at 0 °C for 30 minutes then treated with (*S*)-1-(1-naphthyl)ethylamine (0.85 mL, 5.30 mmol) dropwise. After 30 minutes the reaction was allowed to warm to RT and stirred for 48 hours. All insoluble residues were removed by filtration, the filtrate concentrated to dryness then re-dissolved into CH<sub>2</sub>Cl<sub>2</sub> (150 mL). This solution was washed with 1M HCl (2 x 50 mL), sat. aq. NaHCO<sub>3</sub> (2 x 50 mL) and brine (50 mL) and the organic phase dried over MgSO<sub>4</sub>, filtered and concentrated *in vacuo*. Elution on silica (RediSep® 12g, 0 → 5 % MeOH in DCM) afforded **15S** pure as an off-white solid (0.682 g, 1.39 mmol, 56%); m.p. 154.6 – 155.3 °C; HRMS (*m/z*) (ES<sup>+</sup>) Calculated for C<sub>31</sub>H<sub>28</sub>N<sub>3</sub>O<sub>3</sub> *m/z* = 490.2151 [M + H]<sup>+</sup>. Found *m/z* = 490.2125; <sup>1</sup>H NMR (400 MHz, CDCl<sub>3</sub>) δ : 8.15 – 8.08 (2H, m, naph-CH), 8.02 (2H, s), 7.90 (3H, dd, *J* = 6.6, 3.0 Hz, naph-CH), 7.84 (2H, dd, *J* = 5.9, 3.6 Hz, naph-CH), 7.55 – 7.48 (4H, m, naph-CH), 7.46 – 7.39 (3H, m, naph-CH), 6.00 (2H, app. dd, *J* = 14.6, 7.1 Hz), 1.67 (6H, d, *J* = 6.8 Hz) <sup>13</sup>C NMR (100 MHz, CDCl<sub>3</sub>) δ : 158.37, 137.84, 133.84, 130.71, 130.67, 128.87, 128.40, 126.60, 125.87, 125.29, 122.98, 122.78, 113.23, 45.74, 20.98, 15.23; IR *v*<sub>max</sub> (cm<sup>-1</sup>): 3281, 346, 2970, 2927, 2865, 1654, 1599, 1509, 1448, 1353, 1236, 1135, 996, 799, 774.

### 4-(2,6-Bis(1-(naphthalen-1-yl)ethylcarbamoyl)pyridin-4-yloxy)propane-1-sulphonate (2)

A solution of **3** (1 equiv.) in anhydrous THF (25 mL) was treated with Cs<sub>2</sub>CO<sub>3</sub> (2.5 equiv.) 1,3-propanesultone (0.98 equiv., as a volumetric solution in anhydrous THF) then heated at reflux. The reaction mixture was cooled and concentrated *in vacuo*, then the residue treated with acetone (50 mL) and sonicated for 30 minutes. Residues were isolated by filtration under suction; washed with acetone (250 mL) and Et<sub>2</sub>O (100 mL) then dried under high vacuum and purified on C-18 silica (RediSep®, 4 gram) eluting with 0→100% MeCN in H<sub>2</sub>O, product containing fractions were concentrated *in vacuo* to give caesium salts as white solids. Yield: 71 %; m.p. 220.9 – 222.3 (decomposed at 224 °C); HRMS (*m/z*) (ES<sup>-</sup>) Calculated for C<sub>34</sub>H<sub>32</sub>N<sub>3</sub>O<sub>6</sub>S *m/z* = 61.2020[M – Cs]<sup>-</sup>. Found *m/z* = 610.2017; <sup>1</sup>H NMR (400 MHz, MeOD-*d*<sub>4</sub>) δ: 8.20 (2H, d, *J* = 8.3 Hz, naph-CH), 7.91 (2H, d, *J* = 7.8 Hz, naph-CH), 7.85 – 7.80 (4H, m, naph-CH), 7.66 (2H, d, *J* = 7.0 Hz, naph-CH), 7.58 – 7.37 (6H, m, naph-CH), 6.09 (2H, q,

$J = 6.5$  Hz), 4.36 (2H, t,  $J = 5.64$  Hz), 3.01 (2H, t,  $J = 7.1$  Hz), 2.32 (2H, m), 1.74 (6H, d,  $J = 6.7$  Hz);  $^{13}\text{C}$  NMR (100 MHz, MeOD- $d_4$ )  $\delta$  : 165.87, 162.09, 149.48, 137.05, 132.40, 129.33, 126.94, 126.04, 124.32, 123.72, 123.43, 121.22, 120.85, 109.40, 50.26, 49.87, 43.89, 43.71, 18.27; IR  $\nu_{\text{max}}$  ( $\text{cm}^{-1}$ ): 3300, 2932, 2570, 1638, 1599, 1521, 1393, 1351, 1180, 1137, 1034, 993, 884, 831, 800, 776, 733, 694, 661.

### Photophysical Calculations

Otherwise stated, all measurements were performed at 298 K in methanol or acetonitrile solutions (spectroscopy grade, Aldrich). UV-visible absorption spectra were measured in 1-cm quartz cuvettes on a Varian Cary 50 spectrophotometer. Baseline correction was applied for all spectra. Emission (fluorescence, phosphorescence and excitation) spectra and lifetimes were recorded on a Varian Cary Eclipse Fluorimeter. Quartz cells with a 1 cm path length from Hellma were used for these measurements. The temperature was kept constant throughout the measurements at 298 K by using a thermostated unit block. Phosphorescence lifetimes of the Eu( $^5\text{D}_0$ ) excited state were measured in both water/deuterated water or methanol/deuterated methanol solutions in time-resolved mode at 298 K. They are averages of three independent measurements, which were made by monitoring the emission decay at 616 nm, which corresponds to the maxima of the Eu(III)  $^5\text{D}_0 \rightarrow ^7\text{F}_2$  transition, enforcing a 0.1 ms delay, and were analyzed using Origin 7.5®. The number of water molecules directly bounded to Eu(III) center ( $q$  value) was determined according to the equation developed by Parker *et al* [1]:

$$q = A(\tau_{\text{O-H}}^{-1} - \tau_{\text{O-D}}^{-1}) \quad (1),$$

where  $\tau_{\text{O-H}}$  is the life-time water or methanol solutions,  $\tau_{\text{O-D}}$  is the life-time measured in deuterated water or deuterated methanol solutions.

The quantum yields ( $Q_{\text{rel}}^{\text{Eu,L}}$ ) were measured by relative method [2,3] using  $\text{Cs}_3[\text{Eu}(\text{dpa})_3] \cdot 9\text{H}_2\text{O}$  complex in 0.1 M Tris buffer (pH = 7.45) ( $Q_{\text{abs}}^{\text{Eu}} = 24.0 \pm 2.5$  %) [4] as

a standard with known quantum yield, to which the absorbance and emission intensity of the sample are compared according to:

$$Q_{rel}^{Eu,L} = \frac{Q_x}{Q_r} = \frac{E_x}{E_r} \times \frac{A_r(\lambda_r)}{A_x(\lambda_x)} \times \frac{I_r(\lambda_r)}{I_x(\lambda_x)} \times \frac{n_x^2}{n_r^2} \quad (2),$$

where subscript  $r$  – reference and  $x$  – sample;  $E$  – integrated luminescence intensity;  $A$  – absorbance at the excitation wavelength;  $I$  – intensity of the excitation light at the same wavelength,  $n$  – refractive index of the solution. The estimated error for quantum yields is  $\pm 10\%$ .

$\tau_R$  lifetime was obtained using equation (3):

$$\frac{1}{\tau_R} = A_{MD,0} \cdot n^3 \cdot \left( \frac{I_{tot}}{I_{MD}} \right) \quad (3),$$

where  $n$  is the refractive index of the solvent,  $A_{MD,0}$  is the spontaneous emission probability for the  ${}^5D_0 \rightarrow {}^7F_1$  transition *in vacuo*, and  $I_{tot}/I_{MD}$  is the ratio of the total area of the corrected Eu(III) emission spectrum to the area of the  ${}^5D_0 \rightarrow {}^7F_1$  band ( $A_{MD,0} = 14.65 \text{ s}^{-1}$ ).[5].

The quantum yield of the luminescence step ( $\Phi_{Ln}^{Ln}$ ) expresses how well the radiative process complete with non-radiative processes.

$$\Phi_{Ln}^{Ln} = \frac{\tau_{obs}}{\tau_R} \quad (4),$$

The efficiency of lanthanide sensitization ( $\eta_{sens}$ ) is the ratio between  $\Phi_{tot}$  (determined experimentally) and  $\Phi_{Ln}^{Ln}$  (see equation (4)):

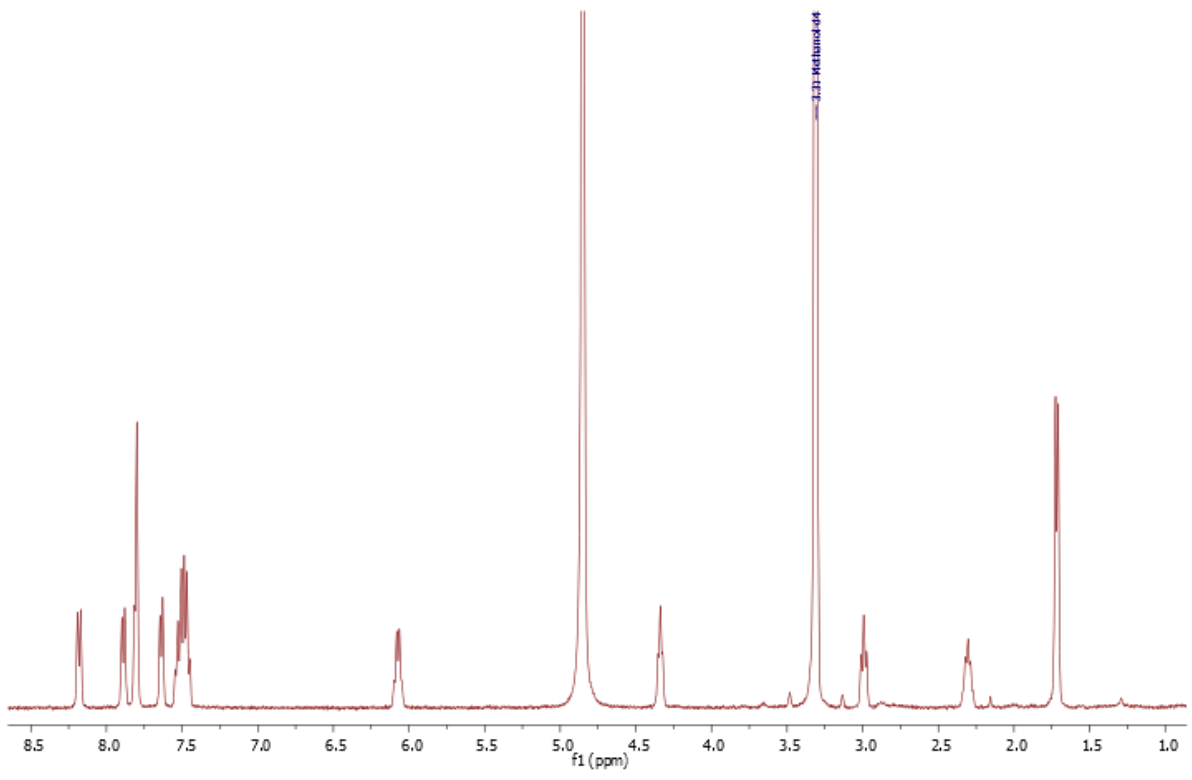
$$\eta_{sens} = \frac{\Phi_{tot}}{\Phi_{Ln}^{Ln}} \quad (5).$$

Circular dichroism (CD) spectra were recorded in methanol solution on a Jasco J-810-150S spectropolarimeter. Circularly polarised luminescence (CPL) spectra were recorded by Dr. R. Peacock at the University of Glasgow. Excitation of Eu(III) (560-581nm) was accomplished by using a Coherent 599 tunable dye laser (0.03 nm resolution) with argon ion laser as a pump source. Calibration of the emission monochromator was accomplished by passing scattered

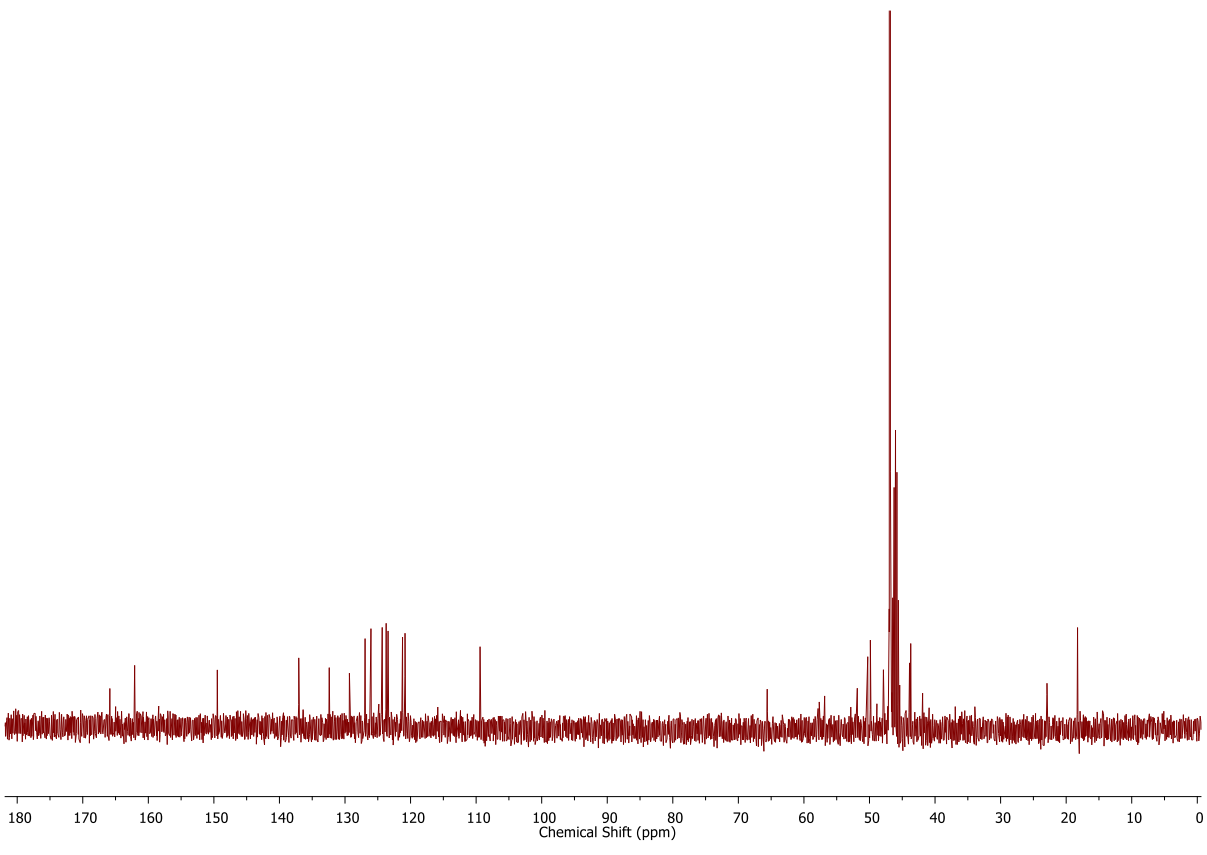
light from a low power HeNe laser through the detection system. The optical detection system consisted of a photoelastic modulator (PEM, Hinds Int.) operating at 50 kHz and a linear polarizer, which together act as a circular analyzer, followed by a long pass filter, focusing lens and a 0.22 m double monochromator. The emitted light was detected by a cooled EM1-9558QB photomultiplier tube operating in photon counting mode. The 50 KHz reference signal from the photoelastic modulator was used to direct the incoming pulses into two separated counters. An up counter, which counts every photon pulse and thus is a measure of the total luminescence signal  $I = I_{\text{left}} + I_{\text{right}}$ , and an up/down counter, which adds pulses when the analyzer is transmitting to the left circularly polarized light and subtracts pulses when the analyzer is transmitting right circularly polarized light. The second counter provides a measure of the differential emission intensity  $\Delta I = I_{\text{left}} - I_{\text{right}}$ .

## References

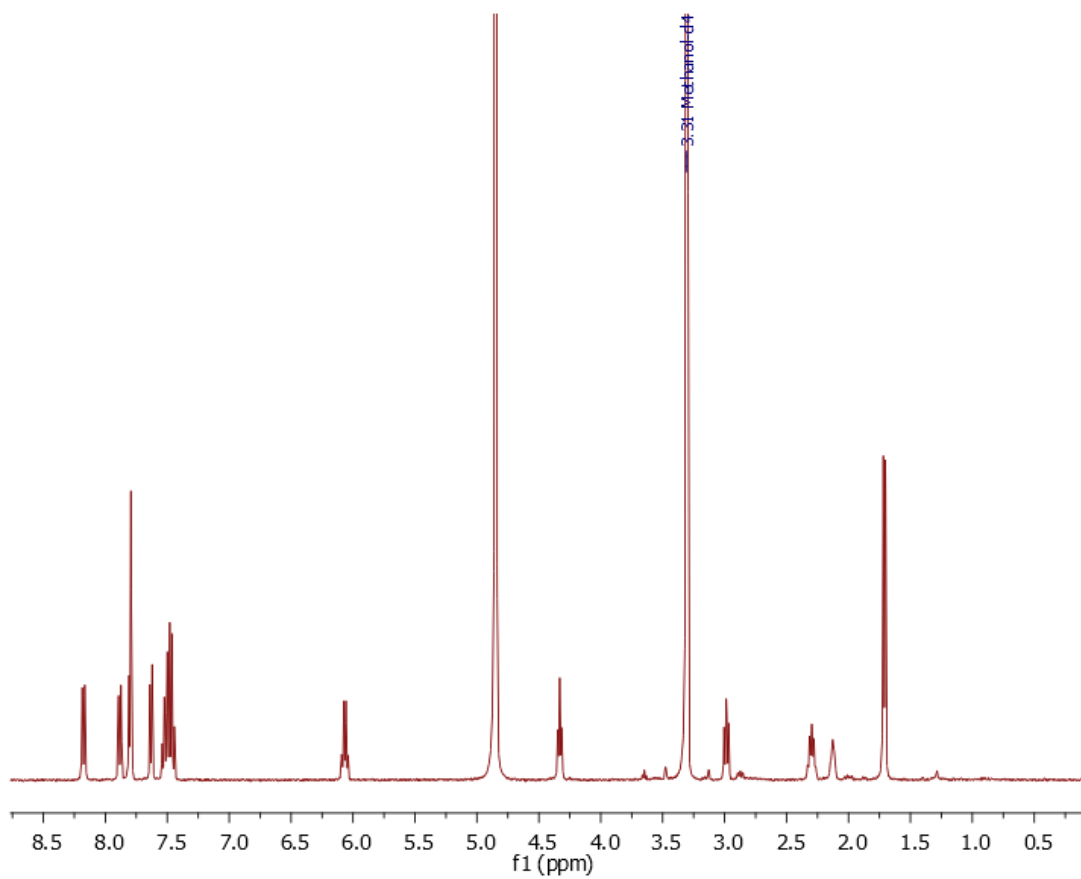
- [1] A. Beeby, I.M. Clarkson, R.S. Dickins, S. Faulkner, D. Parker, L. Royle, A.S. de Sousa, J.A.G. Williams, M. Woods, *J. Chem. Soc., Perkin Trans. 2* **1999**, 493-503.
- [2] G.F. de Sá, L. Nunez, Z.M. Wang, G.R. Choppin, *J. Alloys Comp.* **1993**, 196, 17-23.
- [3] J.N. Demas, G.A. Crosby, *J. Phys. Chem.* **1971**, 75, 991-1024.
- [4] A.-S. Chauvin, F. Gumy, D. Imbert, J.-C. G. Bünzli, *Spectroscopy Lett.* **2004**, 37(5), 517-532; Erratum: *Spectroscopy Lett.* **2007**, 40, 193.
- [5] M. H. V. Werts, R. T. F. Jukes, J. W. Verhoven, *Phys. Chem. Chem. Phys.* **2002**, 4, 1542-1548.



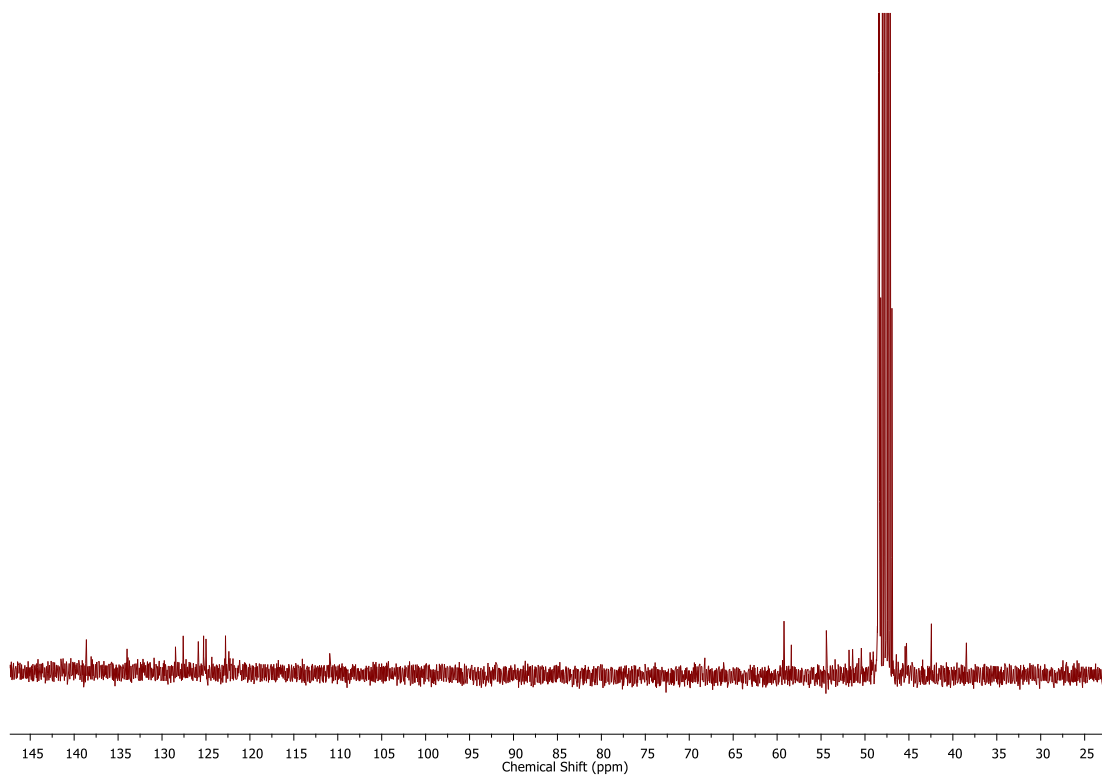
**S1**  $^1\text{H}$  NMR spectrum of **2(S,S)** recorded in  $\text{MeOD-}d_4$



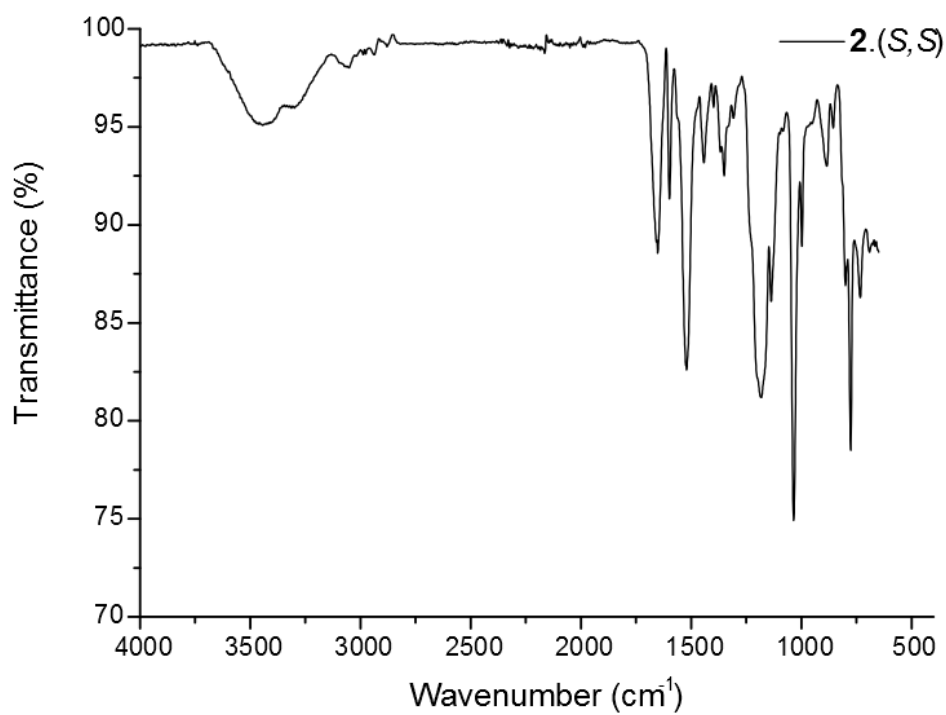
**S2**  $^{13}\text{C}$  NMR spectrum of **2(S,S)** recorded in  $\text{MeOD-}d_4$



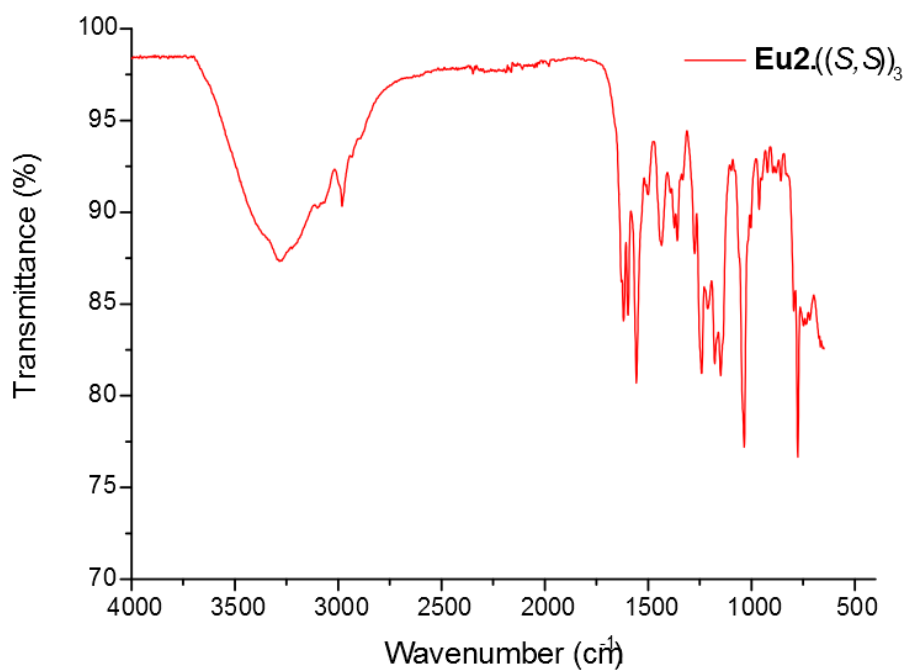
**S3**  $^1\text{H}$  NMR spectrum of 2(R,R) recorded in MeOD- $d_4$



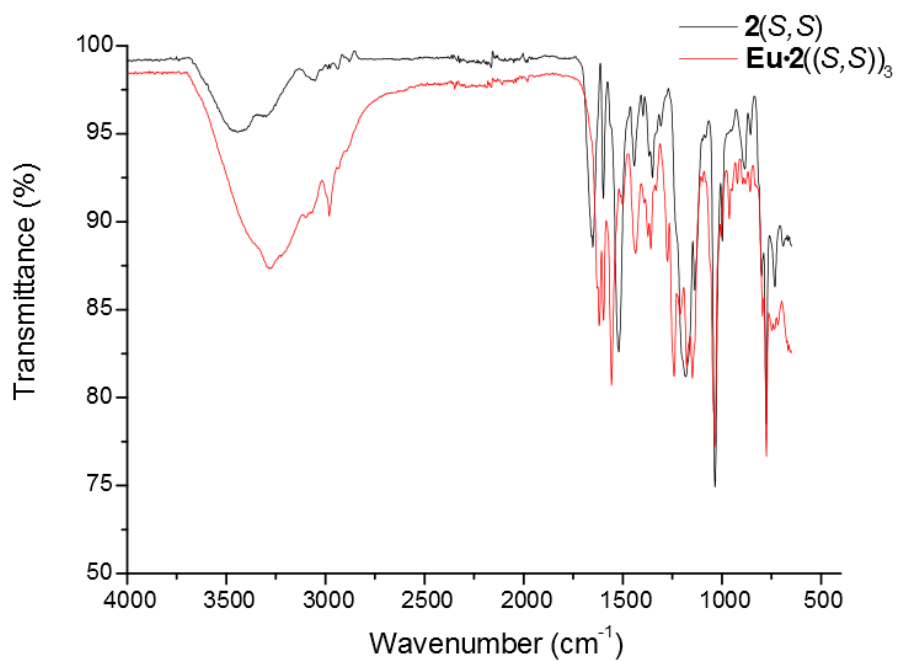
**S4**  $^{13}\text{C}$  NMR spectrum of 2(R,R) recorded in MeOD- $d_4$



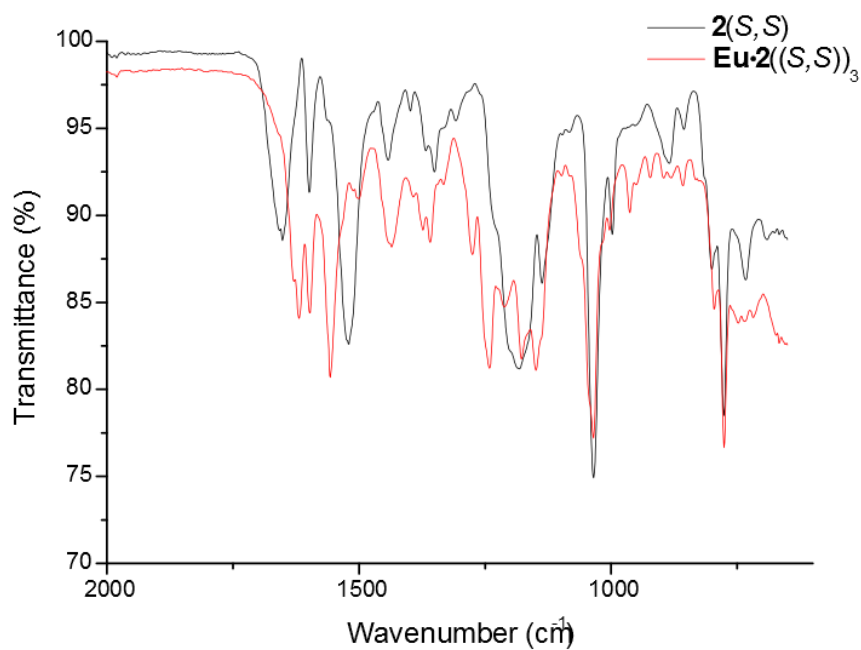
S5 IR spectrum of **2(S,S)**



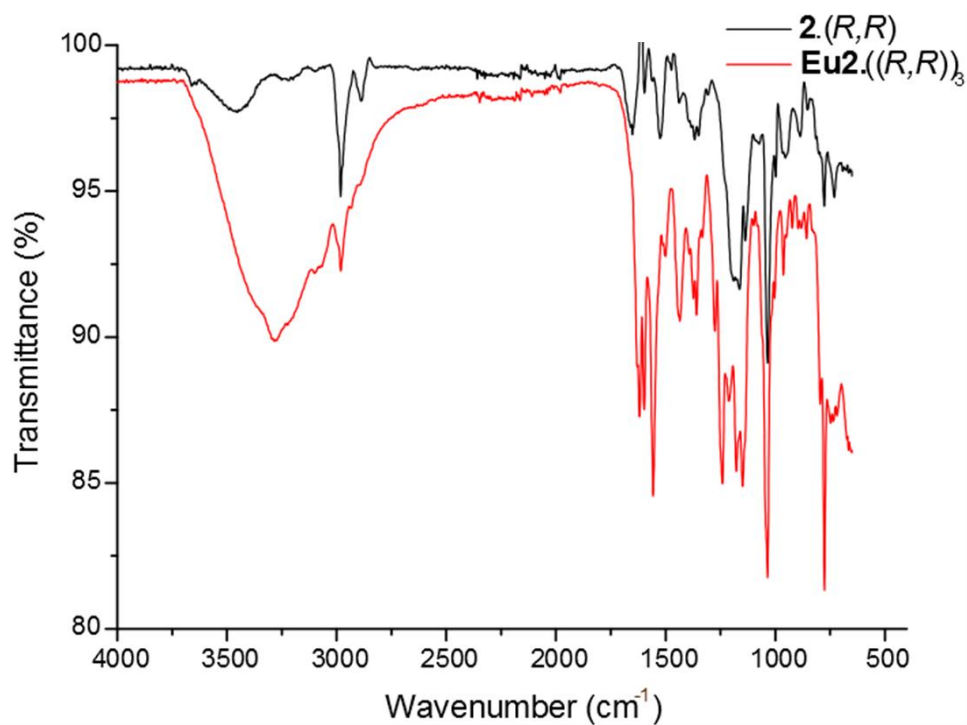
S5 IR spectrum of **Eu.<sub>2</sub>[(S,S)<sub>3</sub>]**



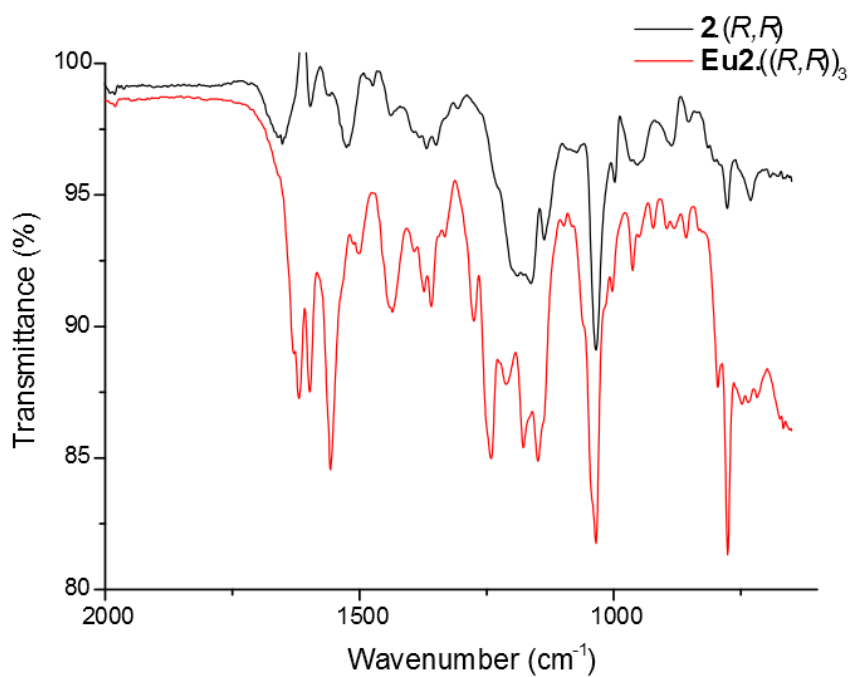
**S5** Overlaid IR spectra of **Eu**·**2**·(**S,S**)<sub>3</sub> and **2**·(**S,S**)



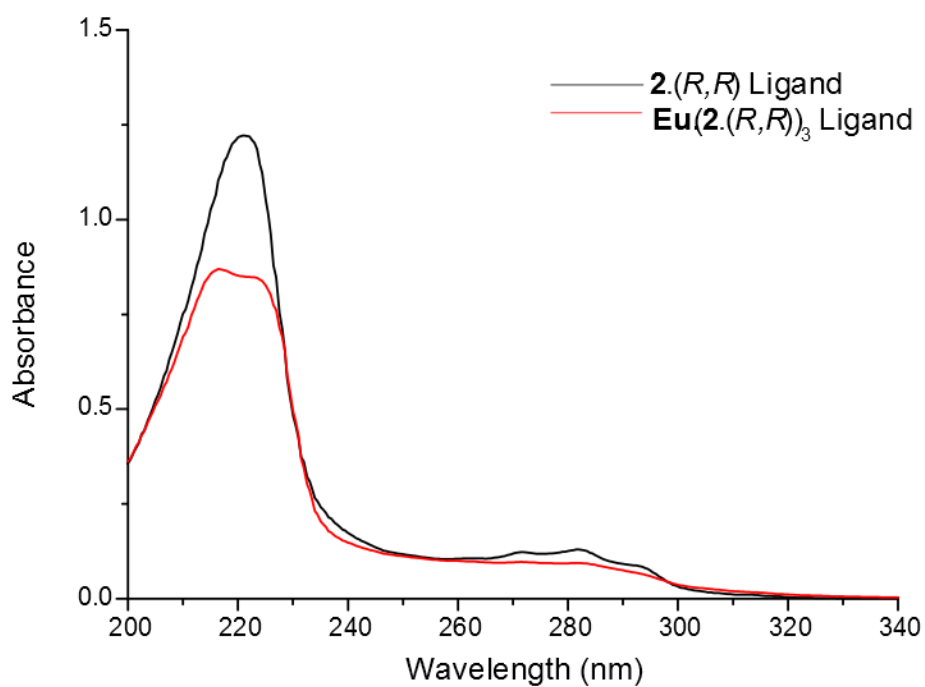
**S6** Zoomed region of overlaid IR spectra of **Eu**·**2**·(**S,S**)<sub>3</sub> and **2**·(**S,S**) showing key carbonyl stretching shifts upon Eu(III) complexation



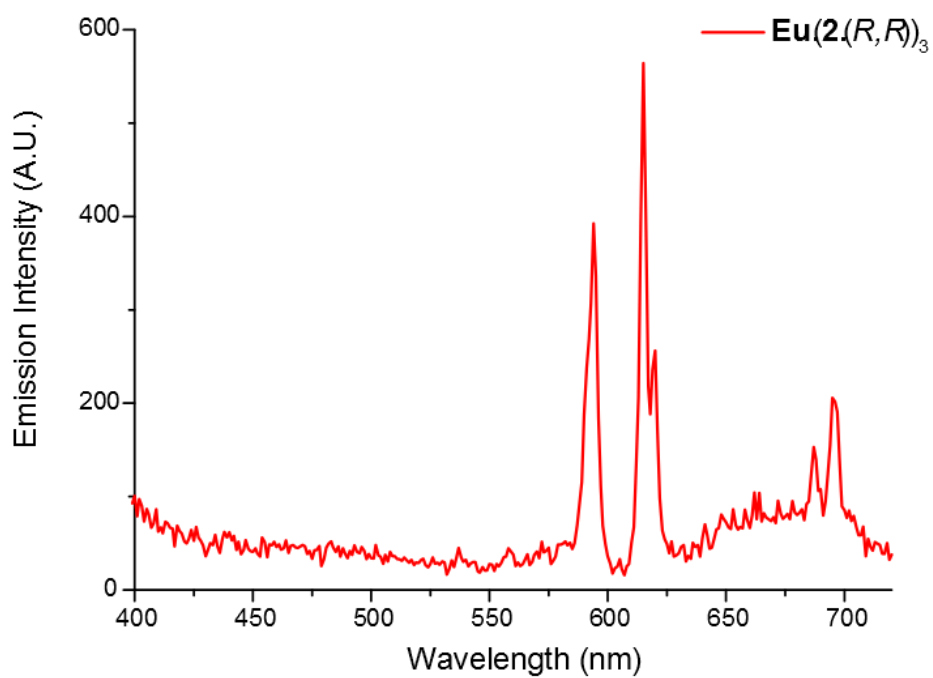
S7 Overlaid IR spectra of  $\text{Eu} \cdot [2.(R,R)]_3$  and  $2.(R,R)$



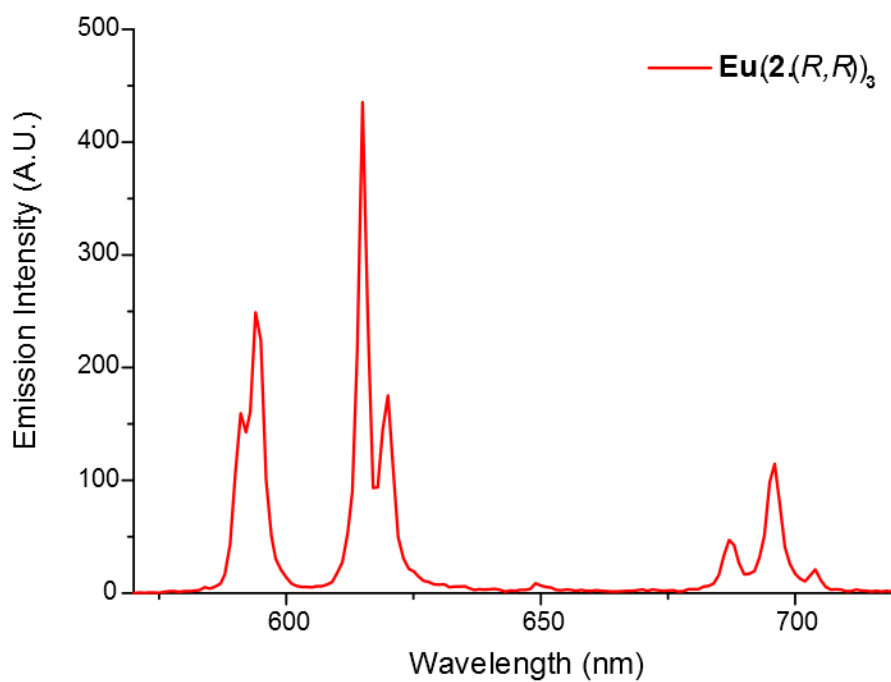
S8 Zoomed region of overlaid IR spectra of  $\text{Eu} \cdot [2.(R,R)]_3$  and  $2.(R,R)$  showing key carbonyl stretching shifts upon Eu(III) complexation



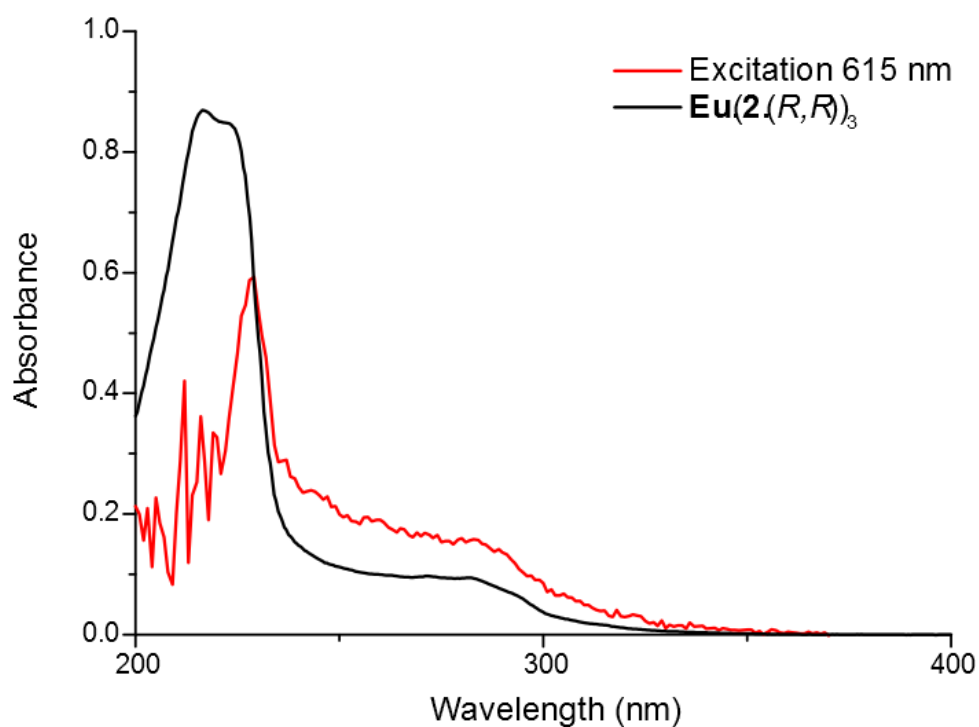
**S9** Overlaid UV-Vis absorbance spectra of **2.(R,R)** and **Eu·[2.(R,R)]<sub>3</sub>**



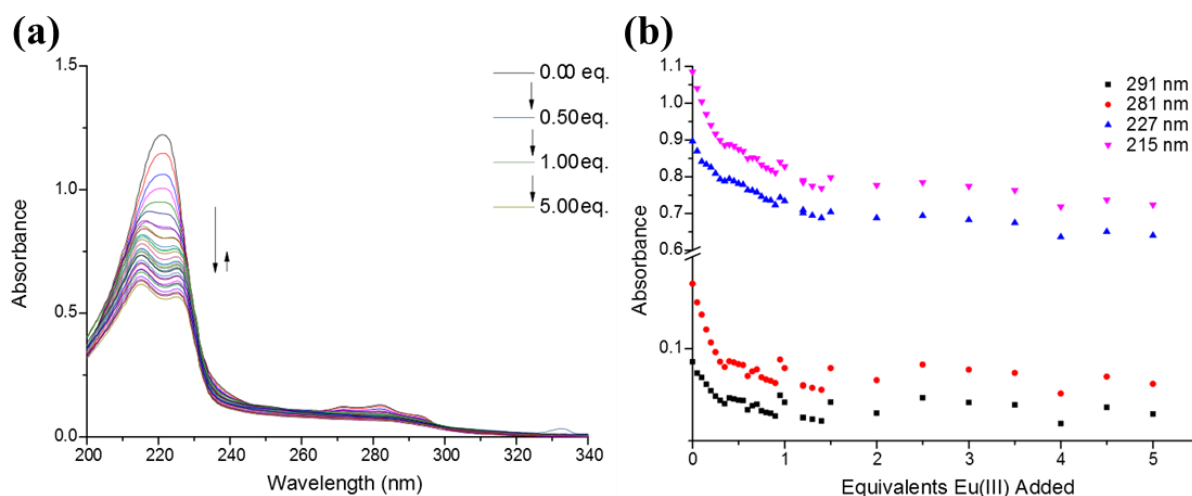
**S10** Fluorescence emission spectrum from **Eu·[2.(R,R)]<sub>3</sub>** showing Eu(III) centred emission



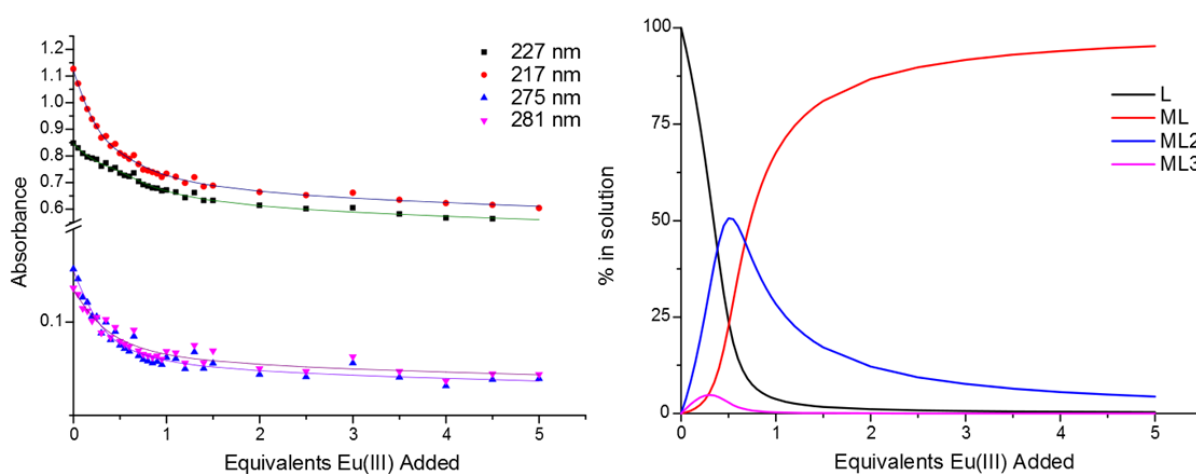
**S11** Time-gated luminescence (phosphorescence mode) spectra from  $\text{Eu} \cdot [\mathbf{2} \cdot (R,R)_3]_3$  showing sensitised Eu(III)-centred emission



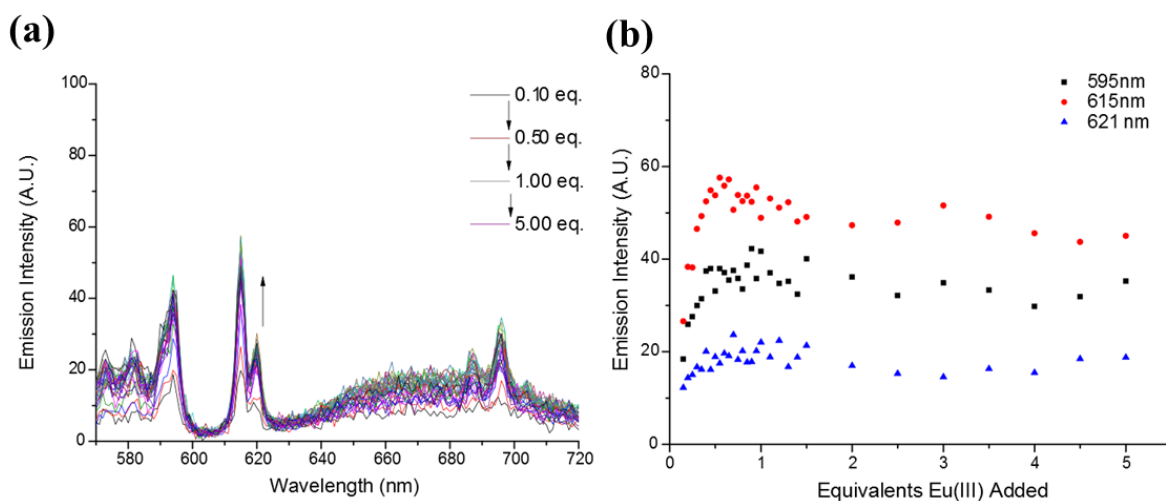
**S12** Overlaid absorbance profile of  $\text{Eu} \cdot [\mathbf{2} \cdot (R,R)_3]_3$  and the excitation spectrum of 615 nm emission in phosphorescence mode.



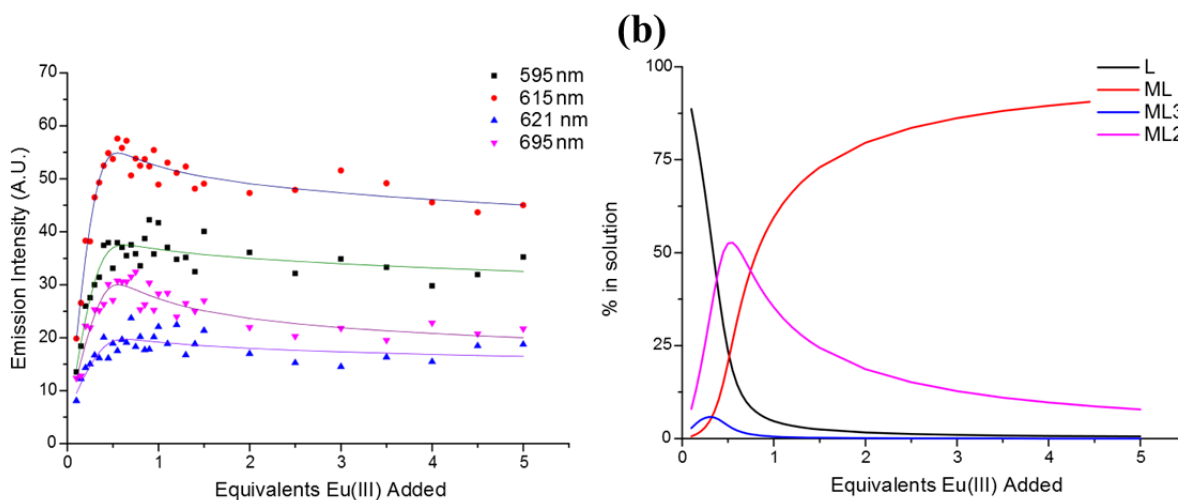
**S13** UV-Visible Titration of **2.(R,R)** (a) overlaid spectra of additions of Eu(III) as Eu(OTf)<sub>3</sub> to **2(R,R)** at  $c = 1 \times 10^{-5}$  (b) Spectral changes at various wavelengths of interest (291, 281, 227 and 215 nm) upon sequential additions of Eu(OTf)<sub>3</sub>.



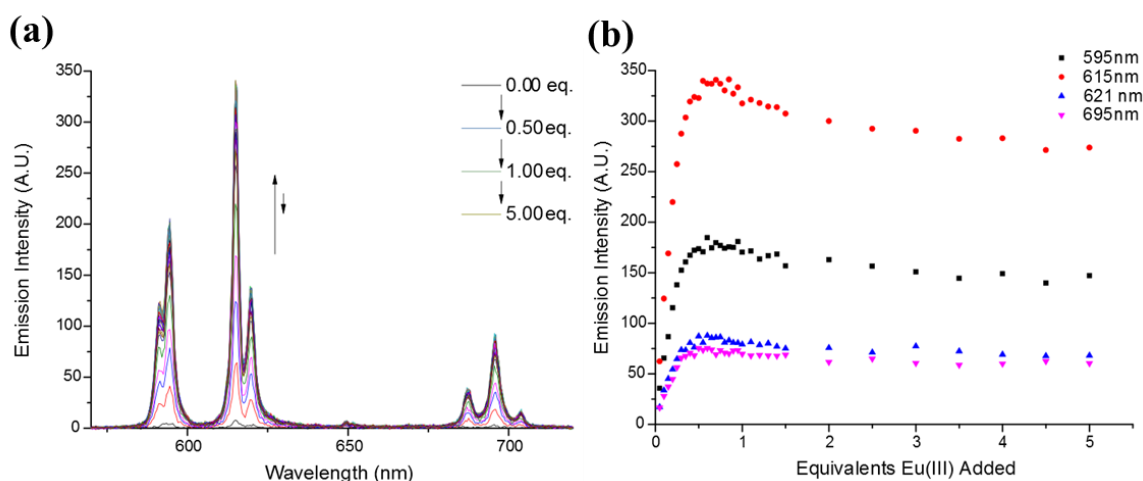
**S14** Fitting results of UV-Visible Titration of **2.(R,R)** with Eu(OTf)<sub>3</sub> (a) Spectral changes at various wavelengths (points, S15b) and their calculated fits from non-linear regression analysis in ReactLab EQUILIBRIA® (b) Generated speciation diagram from regression analysis of UV-changes.



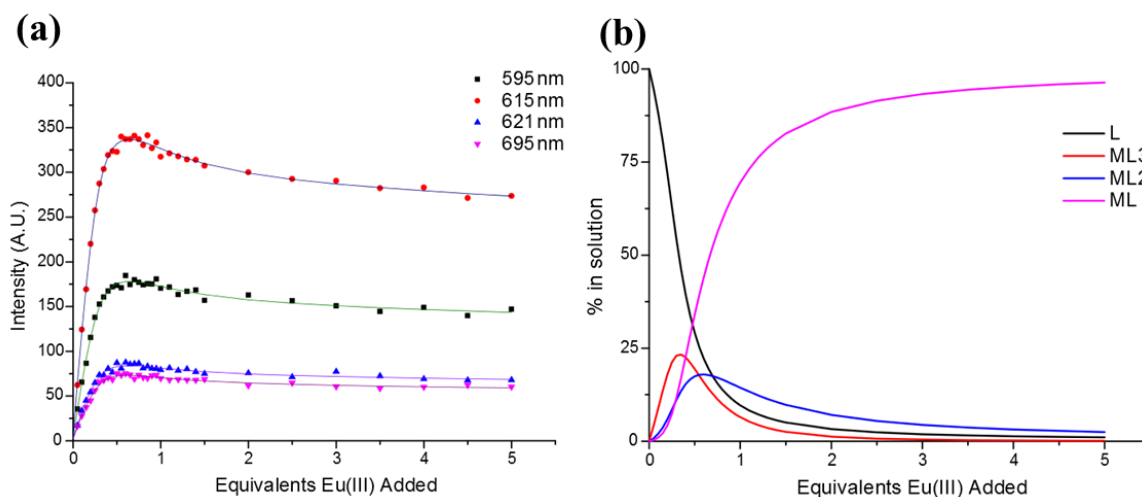
**S15** Fluorescence titration with low signal:noise ratio for **2.**(*R,R*) with  $\text{Eu}(\text{OTf})_3$  at  $c = 1 \times 10^{-5}$  M in water **(a)** overlaid spectra of additions of  $\text{Eu}(\text{III})$  as  $\text{Eu}(\text{OTf})_3$  to **2.**(*R,R*) at  $c = 1 \times 10^{-5}$  **(b)** Spectral changes at various wavelengths of interest (595 ( $J=1$ ), 615 and 621 ( $J=2$ ) nm) upon sequential additions of  $\text{Eu}(\text{OTf})_3$ .



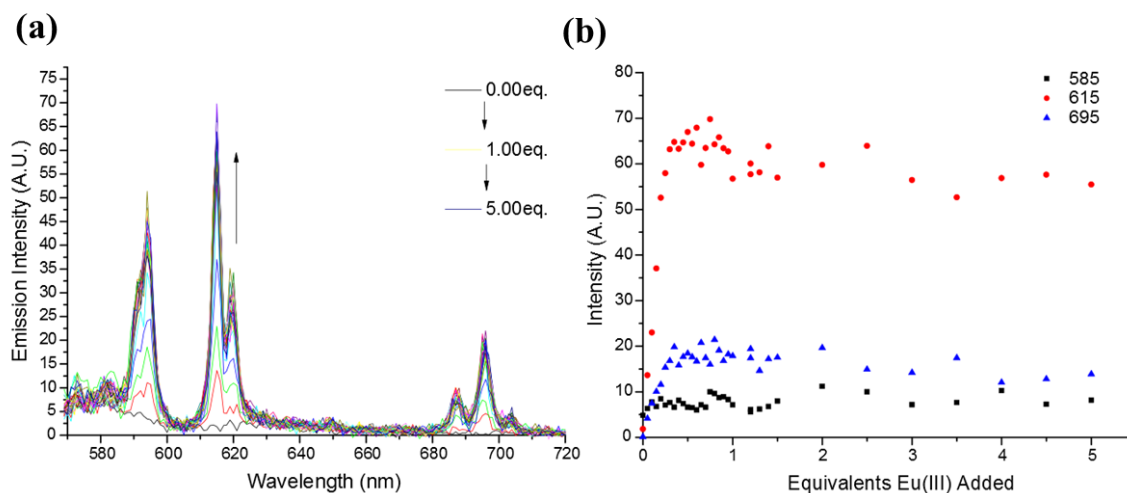
**S16** Fitting results of Fluorescence Titration of **2.**(*R,R*) with  $\text{Eu}(\text{OTf})_3$  **(a)** Spectral changes at various wavelengths (points, S15b) and their calculated fits from non-linear regression analysis in ReactLab EQUILIBRIA® **(b)** Generated speciation diagram from regression analysis of UV-changes.



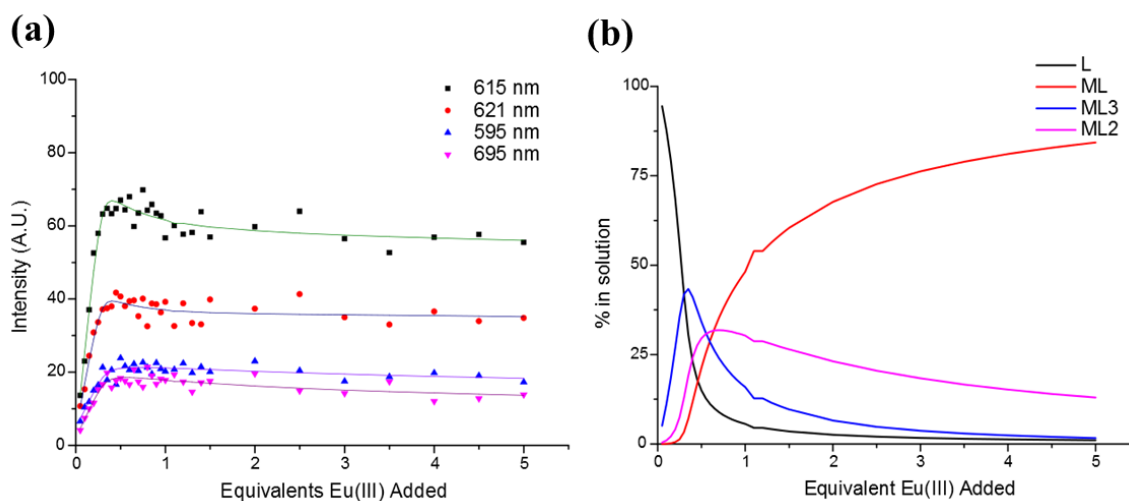
**S17** Time-gated luminescence (phosphorescence mode) titration with high signal:noise ratio for **2.(R,R)** with  $\text{Eu}(\text{OTf})_3$  at  $c = 1 \times 10^{-5}$  M in water (a) overlaid spectra of additions of  $\text{Eu}(\text{III})$  as  $\text{Eu}(\text{OTf})_3$  to **2.(R,R)** at  $c = 1 \times 10^{-5}$  (b) Spectral changes at various wavelengths of interest (595 ( $J=1$ ), 615, 621 ( $J=2$ ) nm and 695 ( $J=3$ )) upon sequential additions of  $\text{Eu}(\text{OTf})_3$ .



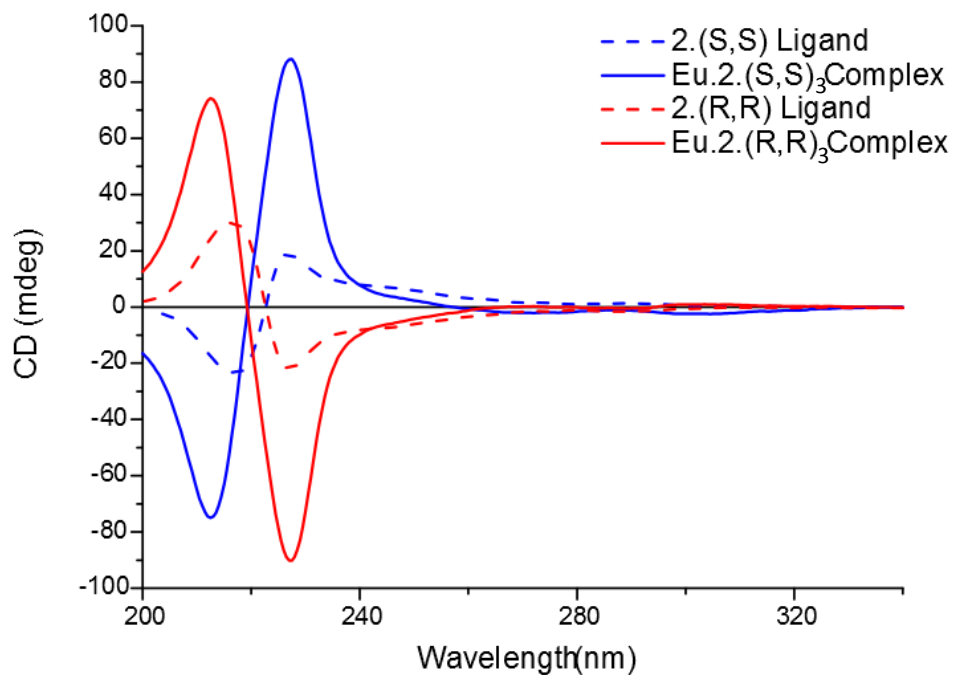
**S18** Fitting results of time-gated luminescence (phosphorescence mode) titration of **2.(R,R)** with  $\text{Eu}(\text{OTf})_3$  (a) Spectral changes at various wavelengths (points, S15b) and their calculated fits from non-linear regression analysis in ReactLab EQUILIBRIA® (b) Generated speciation diagram from regression analysis of UV-changes.



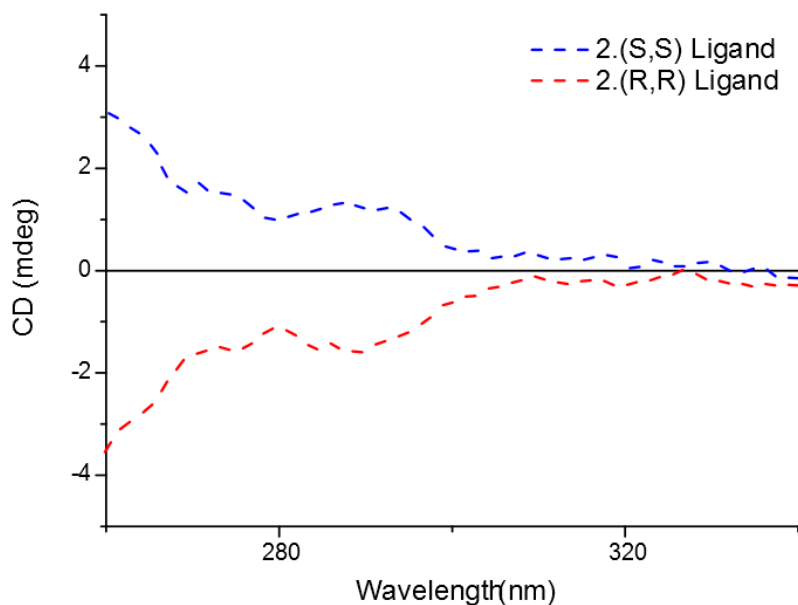
**S19** Fluorescence titration with low signal:noise ratio for **2**.(*S,S*) with  $\text{Eu}(\text{OTf})_3$  at  $c = 1 \times 10^{-5}$  M in water (a) overlaid spectra of additions of  $\text{Eu}(\text{III})$  as  $\text{Eu}(\text{OTf})_3$  to **2**.(*S,S*) at  $c = 1 \times 10^{-5}$  (b) Spectral changes at various wavelengths of interest (595 ( $J=1$ ), 615 and 621 ( $J=2$ ) nm ) upon sequential additions of  $\text{Eu}(\text{OTf})_3$ .



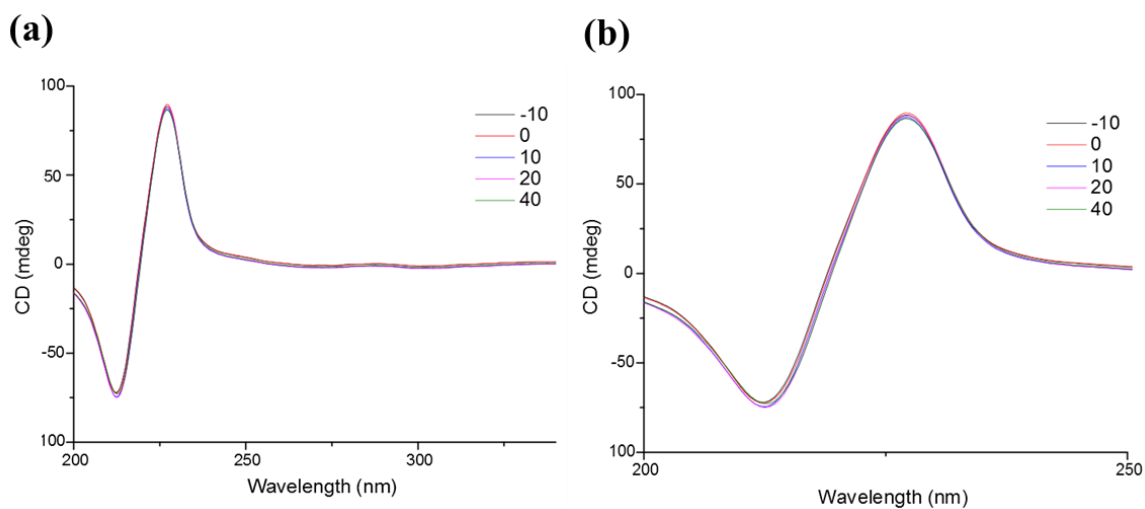
**S20** Fitting results of Fluorescence Titration of **2**.(*R,R*) with  $\text{Eu}(\text{OTf})_3$  (a) Spectral changes at various wavelengths (points, S15b) and their calculated fits from non-linear regression analysis in ReactLab EQUILIBRIA® (b) Generated speciation diagram from regression analysis of UV-changes



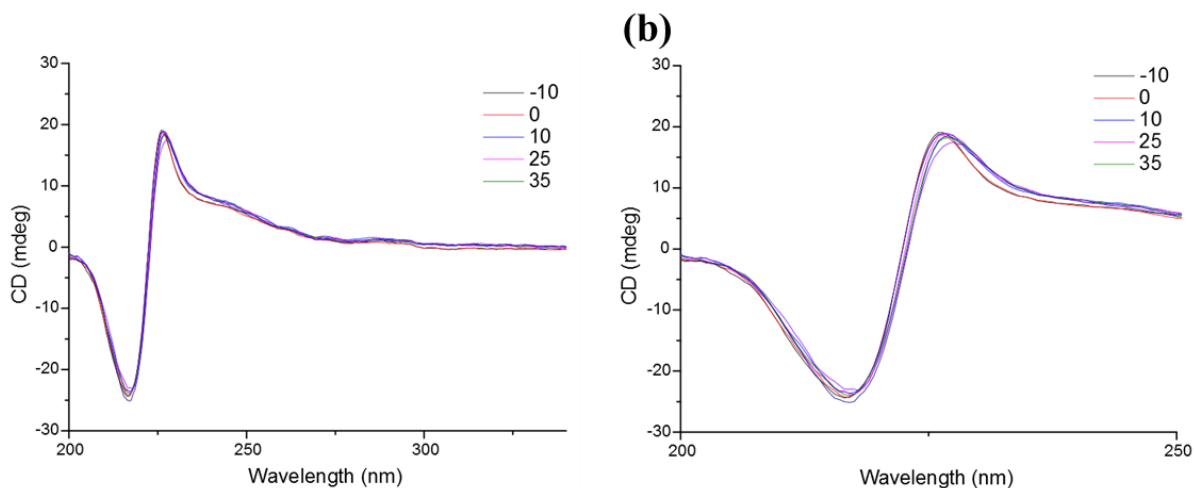
**S21** Overlaid CD spectra of **2.(S,S)** and **2.(R,R)** in water at  $c = 1 \times 10^{-5}$  M (dashed line) and the enhanced CD spectra upon formation of the 3:1 complex (solid line) showing strong bisignate Cotton effect at 200 – 240 nm.



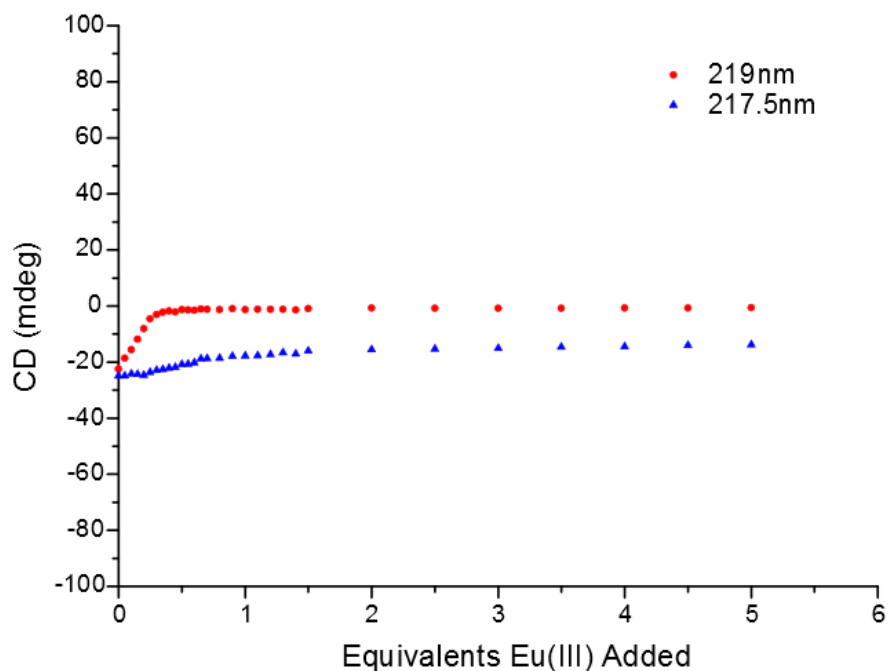
**S22** Overlaid CD spectra (zoomed region) of **2.(S,S)** and **2.(R,R)** in water at  $c = 1 \times 10^{-5}$  M showing weak CD in the naphthyl  $\pi \rightarrow \pi^*$  transitions.



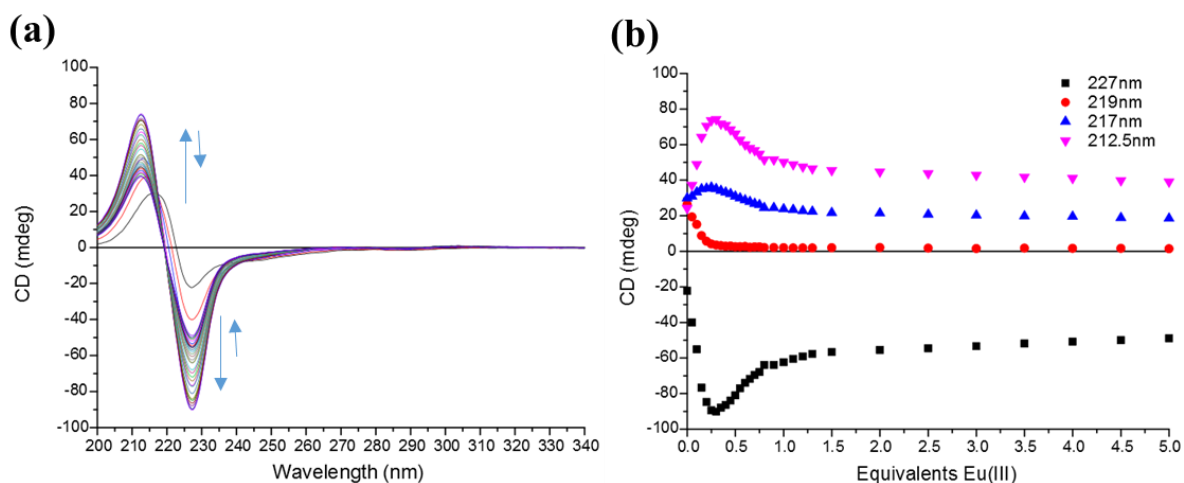
**S23** Variable temperature CD spectra of **Eu.[2.(S,S)]<sub>3</sub>** as representative of both enantiomers. **(a)** Full spectrum of **Eu.[2.(S,S)]<sub>3</sub>** recorded at various temperatures between -10 °C and 40 °C in H<sub>2</sub>O at  $c = 1 \times 10^{-5}$  M **(b)** Zoomed region between of the Cotton effect bands of the CD spectra.



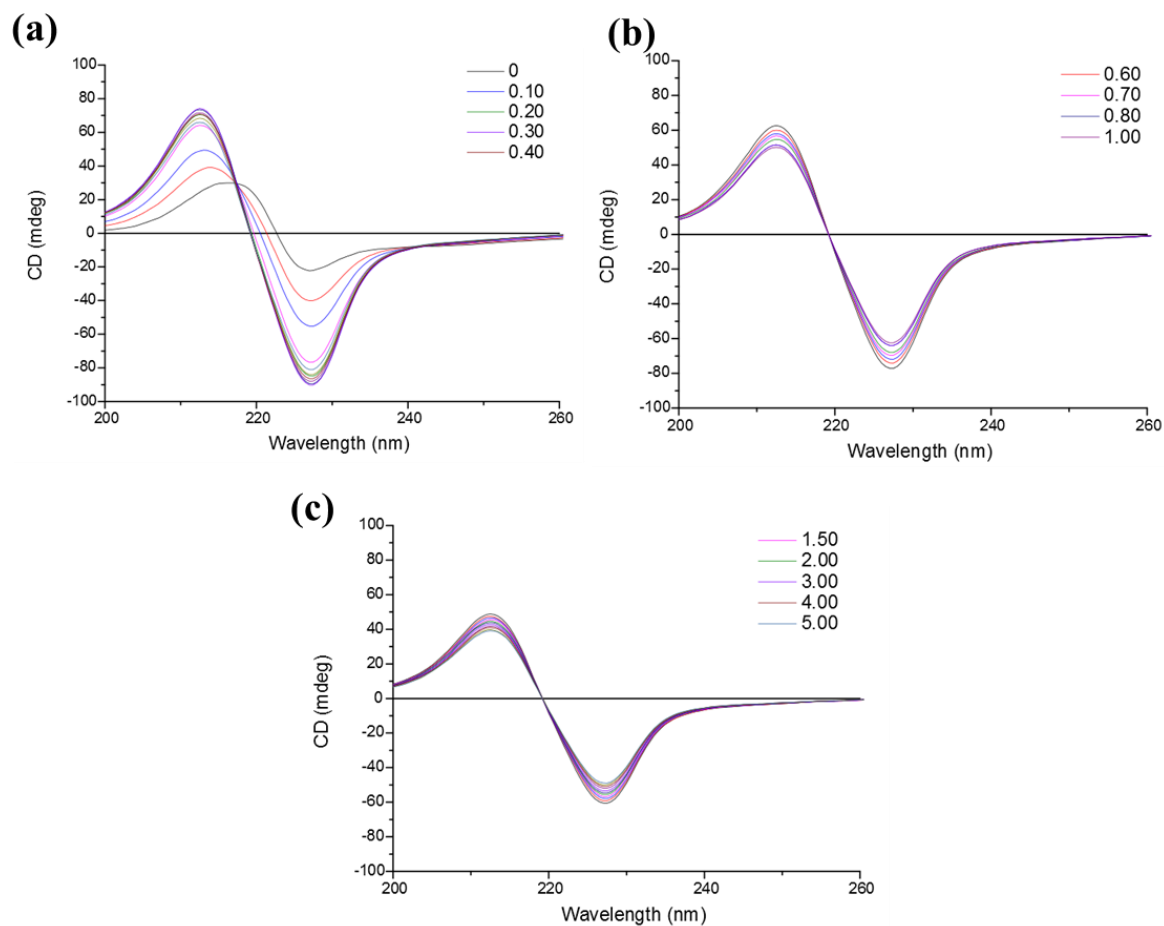
**S24** Variable temperature CD spectra of **2.(S,S)** as representative of both enantiomers. **(a)** Full spectrum of **2.(S,S)** recorded at various temperatures between -10 °C and 35 °C in water at  $1 \times 10^{-5}$  M showing some wavelength shifts **(b)** Zoomed region between of the Cotton effect bands of the CD spectra.



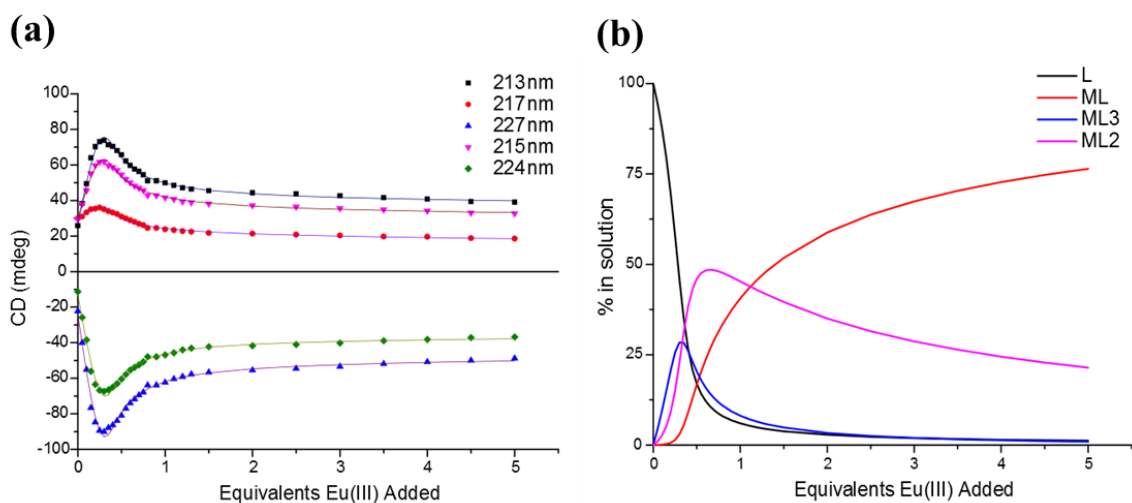
**S25** Spectral changes for two isoeliptic points observed at different stages of the titration of **2**.(*S,S*) with Eu(OTf)<sub>3</sub> 219 nm (0.3→excess) and 217.5 nm (0→0.3 equivalents).



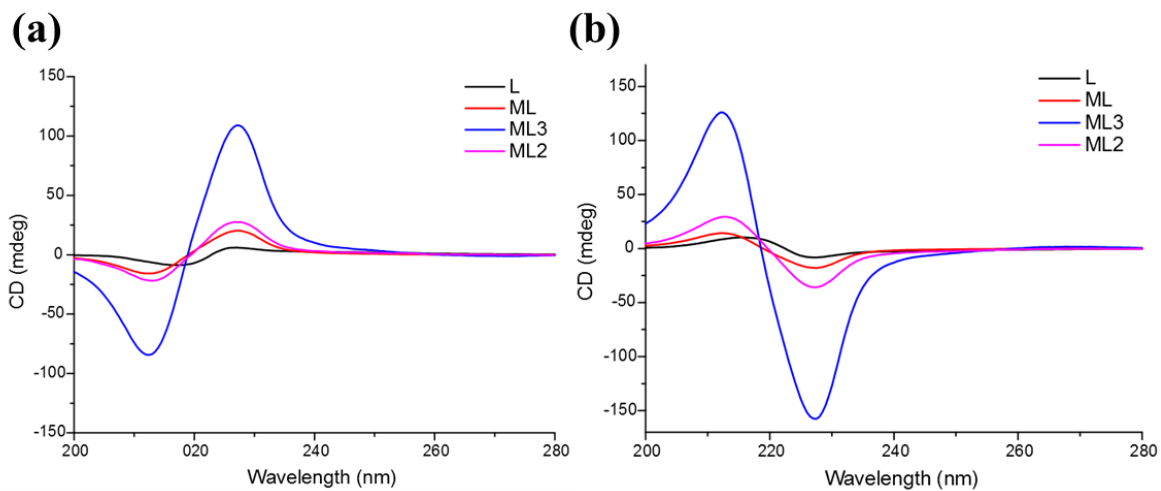
**S26** CD titration of **2**.(*R,R*) with Eu(OTf)<sub>3</sub> in water at  $c = 1 \times 10^{-5}$  M (a) Full spectra from CD titration overlaid (b) Spectral changes in key absorbance wavelengths (227, 219, 217 and 212.5 nm) upon addition of Eu(III).



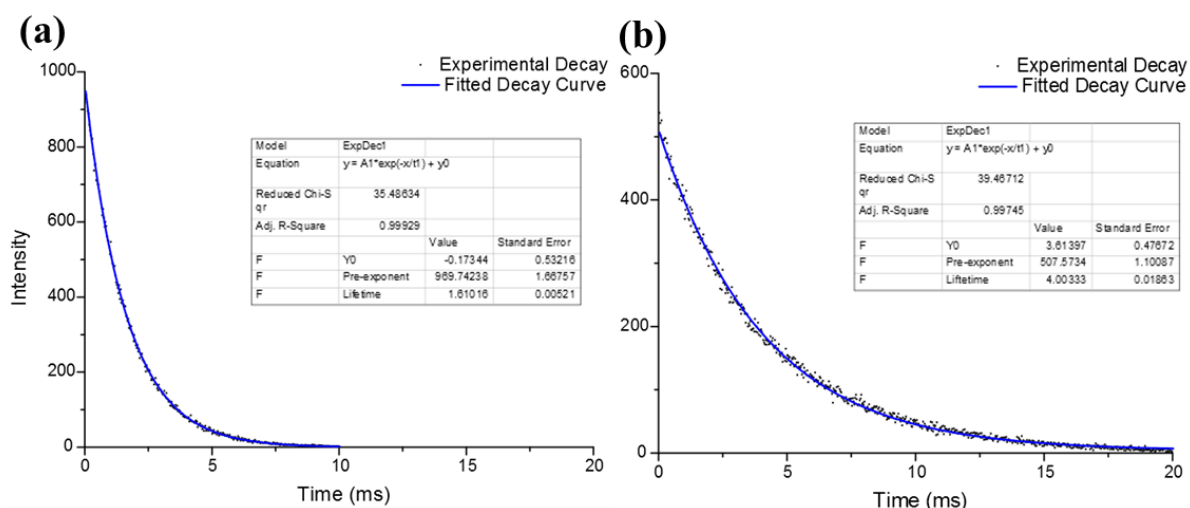
**S27** CD spectra represented between key equivalents of Eu(III) for **2**.(*R,R*) upon additions of Eu(OTf)<sub>3</sub> to **2**.(*R,R*) at  $c = 1 \times 10^{-5}$  M in water showing sequential isoelectric features within the profiles (a) CD spectra recorded between 0→0.4 equivalents Eu(III) (b) CD spectra recorded between 0.5→1.0 equivalents Eu(III) (c) CD spectra recorded between 1.5→5.0 (excess) equivalents Eu(III)



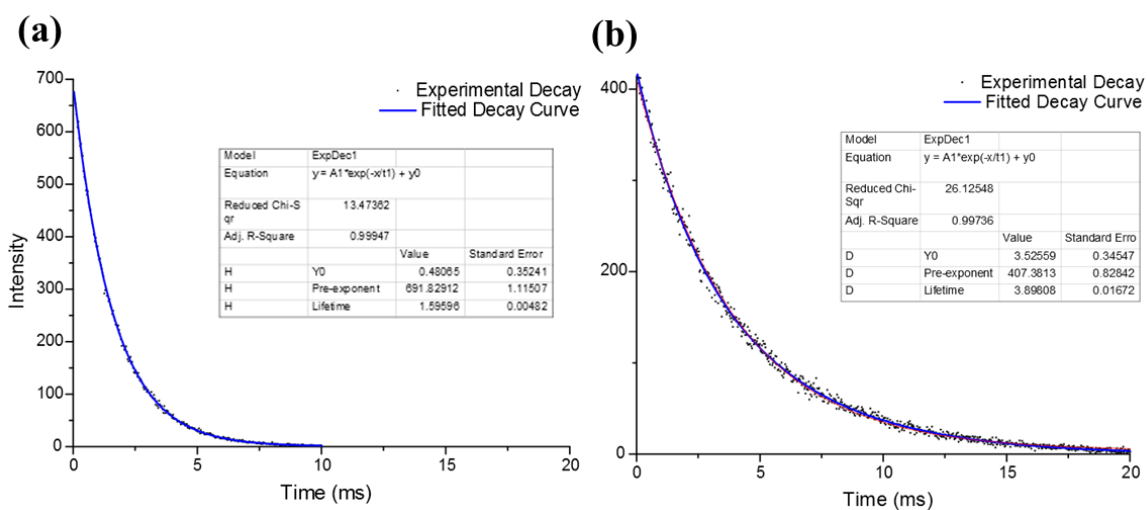
**S28** Fitting results of circular dichroism titration of **2**.(*R,R*) with Eu(OTf)<sub>3</sub> (a) Spectral changes at various wavelengths (points, S26b) and their calculated fits from non-linear regression analysis in ReactLab EQUILIBRIA® (b) Generated speciation diagram from regression analysis of CD-changes.



**S29** (a) Recalculated CD spectra for **2**.(*S,S*) and the 1:1, 2:1 and 3:1 complexes with Eu(III) (b) Recalculated CD spectra from **2**.(*R,R*) and the 1:1, 2:1 and 3:1 complexes with Eu(III)



**S30** Representative experimental luminescence lifetime measurements for  $\text{Eu}.[2.(R,R)]_3$  in (a)  $\text{H}_2\text{O}$  (b)  $\text{D}_2\text{O}$



**S31** Representative experimental luminescence lifetime measurements for  $\text{Eu}.[2.(S,S)]_3$  in (a)  $\text{H}_2\text{O}$  (b)  $\text{D}_2\text{O}$

**S32** Table of experimental luminescence lifetimes ( $\tau$ ) recorded in H<sub>2</sub>O ( $\tau_{\text{H}_2\text{O}}$ ) and D<sub>2</sub>O ( $\tau_{\text{D}_2\text{O}}$ ) from which hydration states ( $q$ , number of bound water molecules) were calculated.

<b>Complex</b>	<b><math>\tau</math> (H<sub>2</sub>O), ms</b>	<b><math>\tau</math> (D<sub>2</sub>O), ms</b>	<b>Horrocks q- value (<math>\pm 0.5</math>)</b>	<b>Parker modified q-value (<math>\pm 0.5</math>)</b>
<b>Eu.[2.(S,S)]<sub>3</sub></b>	1.60 $\pm$ 0.01	3.9 $\pm$ 0.1	0.14(3)	0
<b>Eu.[2.(R,R)]<sub>3</sub></b>	1.61 $\pm$ 0.01	4.0 $\pm$ 0.1	0.14(5)	0